

Numerical Investigation to study the effects of wing flexibility on the store trajectory using MSC CoSim

Varun Palahalli¹, Ganesh Pawar R², Nuza Nigar³, and Praphul T⁴

¹⁻⁴ Hexagon Manufacturing Intelligence, Bangalore, Karnataka – 560043, India

ABSTRACT

Traditional flight testing and wind tunnel testing require expensive resources in terms of time and cost. Safety and cost concerns in the testing of Store separation necessitates the need for a numerical analysis. This paper studies the effect of wing flexibility on store separation trajectory by coupling the fluid dynamics of the airflow with the elastic structural behavior of the wing. The co-simulation is performed by using the MSC CoSim engine that couples structural behavior simulated in MSC Nastran and fluid dynamics simulated in Cradle CFD. The simulation Mach number for this analysis is 0.95. The Eglin Test Model of a flexible wing is used for analysis at Mach number 0.95. The objective of the paper is to investigate the flexibility effects of the wing on the store trajectory. The solver has been validated using a rigid wing of the Eglin Test Model for store drop and then extended to perform the store drop simulation from a flexible wing. The study focuses on comparing the linear and angular displacements of the store dropping from the rigid wing and the flexible wing. It was observed that the trajectory of the store for the flexible wing case showed deviation from the trajectory of the store for the rigid wing

Keywords: Multiphysics, Eglin Test Model, Flexible Wing, Reynolds Averaged Navier Stokes Equation, Fluid-Structure Interaction

1. INTRODUCTION

The separation of the store from the air vehicle is a critical issue in terms of the missile integration process. Whenever a store separates from the aircraft during flight it is essential that it does not come in contact with the aircraft. [1] Traditionally, flight tests were performed to test the store separation, however, they were very time-consuming and often required years to certify a projectile. [2] In the 1960s, wind tunnel testing was done to perform the store separation tests. However, such testing had long lead times and limited accuracy. The method used in such a wind tunnel test is known as the Captive Trajectory System.[3] Since the CTS system had no accuracy in time, it couldn't account for the inherent unsteadiness encountered by the store during separation. The usage of small-scale models often leads to a reduction in accuracy due to the scaling issues.[4] The development of High Parallel Computing and numerical algorithms have paved the path to numerical simulation for store separation. Such numerical modeling and

simulations have reduced the certification cost and increased experimental validity.[5] Trajectories of stores released from internal weapons bays have been shown in recent tests to diverge from predicted paths. Unsteady aerodynamics induced on the store due to wing flexibility results in a change in the trajectory.

2. EGLIN TEST MODEL

The EGLIN test model [3] is made up of three parts that were created using SOLIDWORKS. The first is a delta wing with a constant NACA 64A010 airfoil section and a 45° sweep, the second is a pylon with ogive-shaped leading and trailing edges. The third is a finned store body with a standard missile profile. The wing's trailing edge has no sweep angle and a taper ratio of 0.133. On the store are four identical fins made of a clipped delta wing of a constant NACA 0008 airfoil section with a 45° sweep. Fins have leading and trailing edges with sweep angles of 60 degrees and 0 degrees, respectively. The pylon and the store body are separated by 35.6 mm.

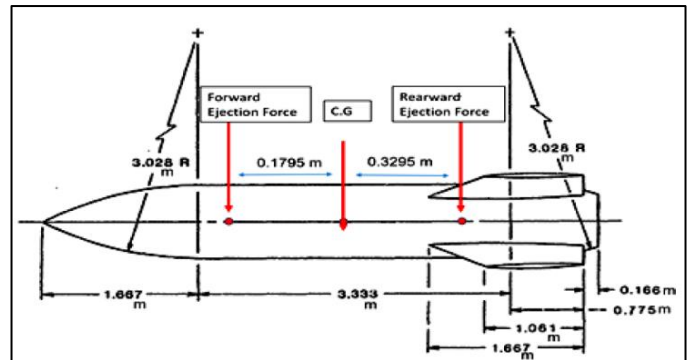


Figure 1: Dimensions of the store [1]

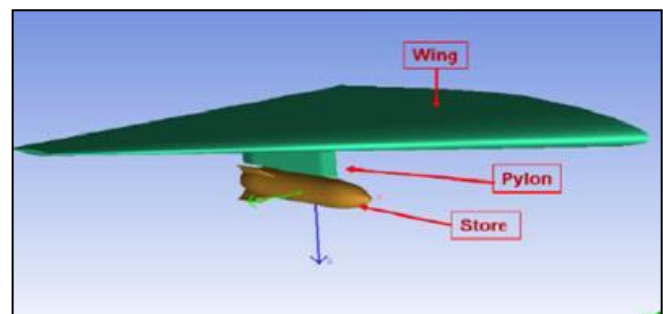


Figure 2: Geometry of Eglin Wing, Pylon and Store [1]

The length and diameter of the store are 3017.5 mm and 508.1 mm, respectively as shown in Figure 1. The store is ejected with a specified force to begin a safe initial separation. The ejector forces act for a duration of 0.052 seconds. Also the store is subjected to aerodynamics and gravity loads. [3] The model orientation is such that the gravity is in the Z direction, the flow is in the negative X direction and the span of the wing is in the Y direction as seen in Figures 2 and 3.

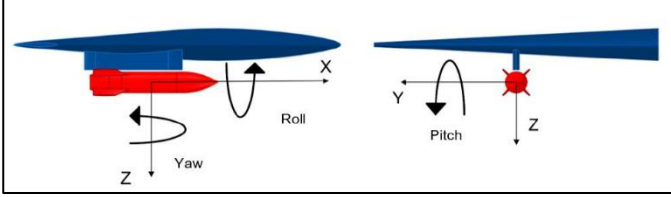


Figure 3: Angular Orientation of the Eglin Test [2]

3. COMPUTATIONAL METHODOLOGY

The study involved validation of the Eglin Test Model of a rigid wing against the paper “Numerical Simulations of Store Separation Trajectories Using the EGLIN Test,” by Y. E. Sunay, E. Gülay, and A. Akgül [3]. The analysis was then extended to study the effect of the flexibility of the wing on the store trajectory.

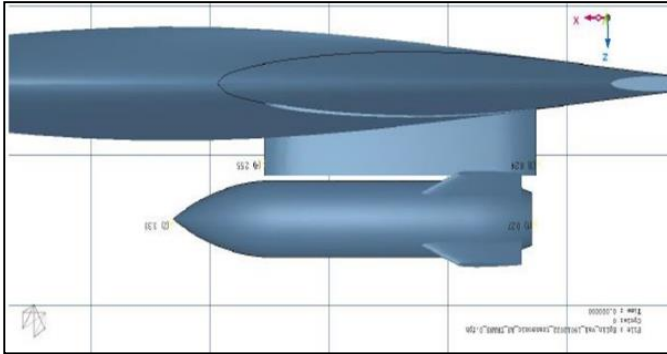


Figure 4: scFLOW Model used in the analysis

3.1 Computational Fluid Dynamics

Unsteady Reynolds Averaged Navier Stokes Equation describes how pressure, temperature, and density are related to a moving fluid. They consist of a set of coupled partial differential equations; one continuity equation for mass conservation, three equations for momentum conservation, and one equation for energy conservation, all of which are time-dependent.

To simulate flows around moving objects, scFLOW employs the ALE (Arbitrary Lagrangian-Eulerian) method, [6] which handles both the moving coordinate system and the fixed coordinate system at the same time. The effect of mesh movement is added to the equation of the fixed coordinate system in the moving region, and the fixed and moving coordinate systems are calculated simultaneously. Moving condition setting for a moving region as well as the selection and setting of the connection method for both static and moving regions are required in the simultaneous calculation with the ALE method. By applying the moving condition to the volume

region containing the object, the moving object is developed. Translation and rotation are examples of settable motions. The static and moving regions can be connected by an overset mesh.

The Eglin Test Model consists of the wing, the pylon, and the store is modeled as shown in Figure 2, to which an external flow domain is added, known as the computational domain where the external flow over the model will be analyzed. The dimensions of the domain are a length and breadth being 747.6 m each. The depth of the domain is 347.6 m. The size of the computational domain must be large enough so as to not have any far field flow perturbation influence on the store. A subdomain domain of length, breadth, and depth of 5.02 m, 2.91 m, and 2.91 m respectively are created and centered on the centre of gravity of the store which is used to create overset mesh over the domain. The total number of mesh elements is 22,01,265. The mesh contains Its spatial hexahedral meshing with prism elements at the walls and polyhedral at the transition between hex and prism elements.

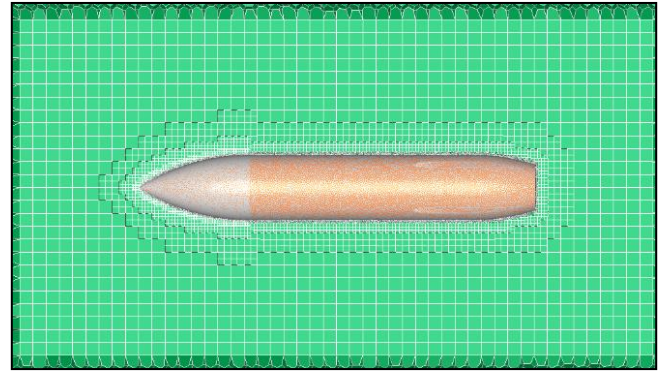


Figure 5: Mesh of the model in scFLOW

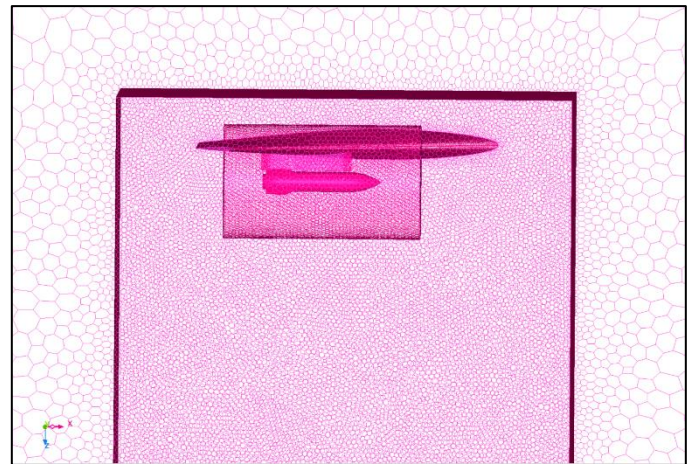


Figure 6: Polyhedral Meshing of the full model in scFLOW

The wing pylon body and the missile body are modeled as obstacles. The fluid around the obstacles is modeled as compressible air at 20 degrees Celsius, due to which the density-based solver is used. The turbulence model employed for this study is the standard k- ϵ model. [7] The k- ϵ model

is a 2-equation closure model which includes two additional transport equations, which are the Turbulence Kinetic Energy k and the Turbulence Dissipation ϵ .

A steady state analysis is performed for the model without the motion initiation of the store to stabilize the solution. The results of the steady-state simulations are adopted as the initialization for the transient state calculation for the store drop trajectory analysis using a rigid wing. The same steady-state simulation is also used for the transient state analysis using CoSim for the flexible wing. For this study, the steady-state simulation was run for 2000 cycles. The default temperature is set at 236.7 K. The flow parameters are shown in Table 1.

Second-order accuracy with a limiter is used for the accuracy of the convective terms for the mass, momentum, energy, turbulence, and diffusion equations. First Order Accuracy of Time Derivative is used. The Least Square Method is used for Gradient Calculation.

The simulation has been performed in the transonic regime. The Mach number under consideration is 0.95. [3] The 6 DOF Parameters used are specified in Table 2.

| Parameters | Value |
|--------------------|-----------------|
| Static temperature | 236.7 K |
| Reference Pressure | 36042 Pa |
| Mach No. | 0.95 |
| Turbulence model | RANS, k-epsilon |
| Time-step | 1e-04 [s] |
| No. of elements | 2.2 million |

Table 1: Flow parameters used in the study [3]

| Parameters | Value |
|-----------------------|-----------------------------|
| Mass | 907.185 kg |
| Center of Mass | 1417.3 mm (aft of STV nose) |
| I_{xx} | 27.1163 kg-m ² |
| I_{yy} | 488.0944 kg-m ² |
| I_{zz} | 488.0944 kg-m ² |
| Forward Ejector Force | 10676.01 N |
| Aft Ejector Force | 42703.0 N |

Table 2: Rigid body dynamic characteristics for the store [3]

3.2 Computational Structural Mechanics

To simulate the flexible wing FEM Model, MSC Nastran is used. This study uses Implicit Non-Linear Analysis.[3] Mid-surfacing is used to represent the wing and pylon and the equivalent model is meshed using shell elements. CTRIA 6 [9], a Higher- Order Quadratic Element, is an isoparametric

triangular shell element, is used for meshing the wing and pylon. The material properties of the Eglin Wing are given in Table 3.

| Parameter | Value |
|-----------------|----------------------------|
| Youngs Modulus | 68.9 E03 MPa |
| Poisson's Ratio | 0.33 |
| Shear Modulus | 25902.256 MPa |
| Density | 2.7 E-09 t/mm ³ |

Table 3: Material Properties of Eglin Wing

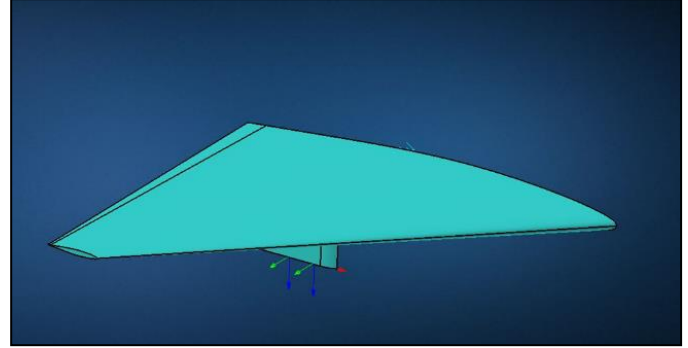


Figure 7: Structure Model developed in MSC Apex

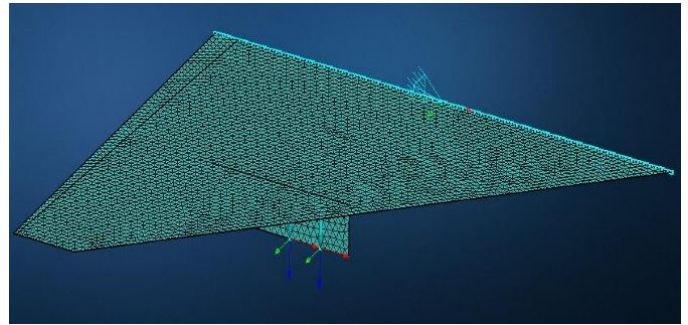


Figure 8: 2D Structure Meshing on Wing and Pylon

An assumed linear isotropic material is used for the flexible structural model in the analysis. The root of the wing has all the 6 DOF constrained. Nodal points for the reaction forces to act on the wing are created corresponding to the location of the ejector forces applied to the store. The wing surface and the structural shell surface are coupled for data exchange in the CoSim engine. The weight of the store is modeled as loads being supported by the ejectors at the pylon, ejector forces are applied on the store, and corresponding equal and opposite reaction forces are applied on the wing pylon as shown in Figures 7 and 8. The store itself is modeled as a rigid body in CFD and is not modeled in the flexible wing FEA model.

3.3 Multiphysics Co-simulation using MSC CoSim.

MSC CoSim[4] creates an interface to replace the arbitrary pressure applied in MSC Nastran with the CoSim search parameters. Interpolation functions map the CFD outputs to the structure and structural outputs to CFD to form a strong, two-

way coupling in real-time. MSC CoSim is used to establish the co-simulation coupling between CFD Solver and Nastran as shown in Figure 9. The two-way coupling happens through the surface where the data mapping region is the upper and lower surface of the wing and the sides of the pylon. The pressure and velocity data are transferred from scFLOW to Nastran and the displacement vector is received from Nastran to scFLOW. The method of mesh deformation is selected as LDC [5] (Linear Displacement Combination).

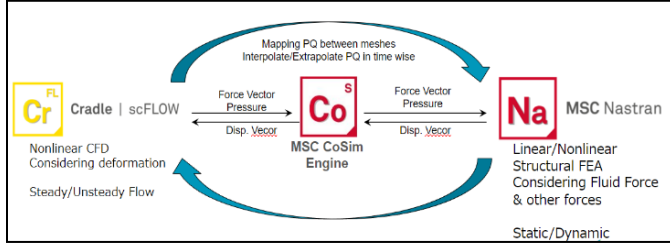


Figure 9: MSC CoSim Data Exchange between MSC Nastran and scFLOW

4. RESULTS AND DISCUSSION

For the flexible wing, wing oscillations are observed upon ejection of the store. The oscillations are caused by the ejection forces that act on the wing. The elasticity of the wing causes oscillations that affect the surrounding fluid, thus altering the store's trajectory. As a result, the trajectory of the store ejecting from the flexible wing shows a deviation when compared to the trajectory of the store ejected from the rigid wing.

X, Y, and Z displacements of the store are shown in Figure 10-12. A small difference in the X trajectory and Y trajectory was observed.

The X trajectory of the store dropping from the flexible wing of assumed stiffness appears to be a closer match to the experimental case which also has some flexibility than the X trajectory of the store dropping from the rigid wing.

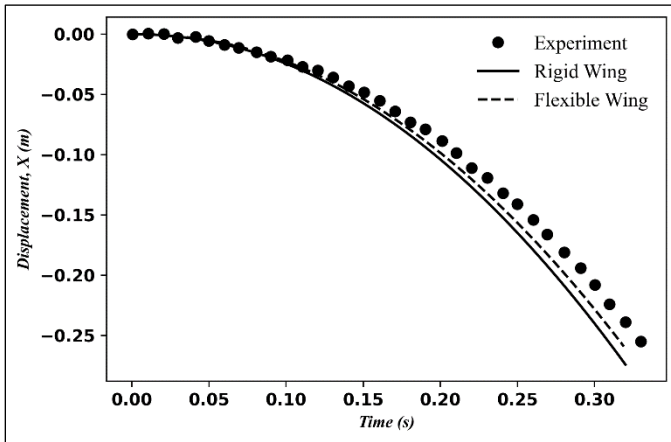


Figure 10: Linear Displacement versus Time graph in X direction comparing Flexible and Rigid Wing

The Y trajectory of the store dropping from the rigid wing appears to be a closer match than the store dropping from the flexible wing.

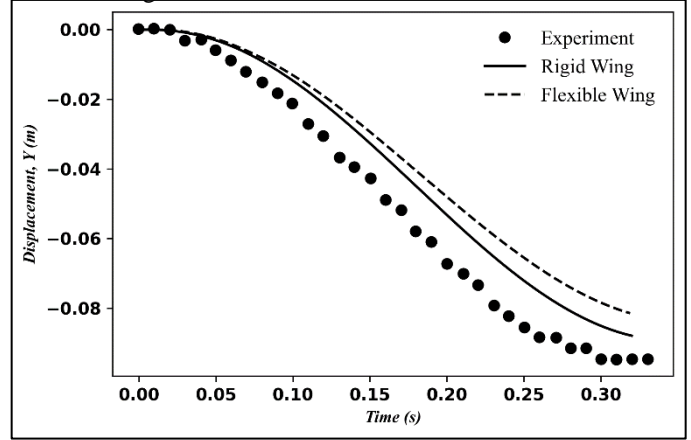


Figure 11: Linear Displacement versus Time graph in Y direction comparing Flexible and Rigid Wing

The effect of the flexibility of the wing on the store's translation in Z is seen to be negligible. The effects of the ejector and gravity forces dominate the effect of the aerodynamic forces in the Z direction. [2] The graph for the store trajectory dropping from the fixed wing as well as the rigid wing is in good agreement with the graph of the experimental data as depicted in Figure 12.

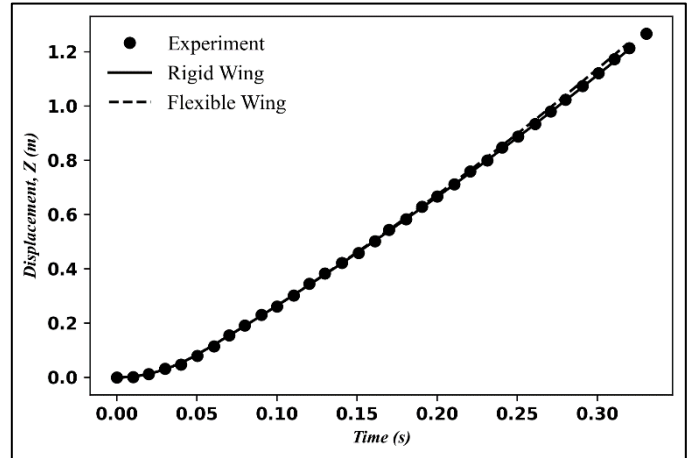


Figure 12: Linear Displacement versus Time graph in Z direction comparing Flexible and Rigid Wing

The store angular orientation is shown in Figure 3. Figure 13-15 compares the store angular orientations with respect to the time of the experimental, rigid, and flexible wing cases.

The pitch-up motion observed in the angular orientation graph for both rigid and flexible wing cases is due to the action of the ejector force. However, with an increase in time, the pitching trend of the flexible wing case differs from that of the rigid wing case. Approximately after 0.15 seconds, the store begins to pitch down as shown in Figure 13. This behavior may be attributed due to the onset of aerodynamic and gravity forces upon store separation.

It is observed from Figure 13 that the pitching angle of the store's trajectory, ejected from the flexible wing is pronounced from that of the rigid and experimental cases. Additionally, the experimental case's pitching angle curve can be seen to lie between that of the rigid wing's store and the flexible wing's. This is inherently due to the experimental wing having flexibility. The marked deviation in the flexible CoSim case's store trajectory is due to the assumed stiffness value owed to the lack of literature stating the exact stiffness or construction of the experimental wing.

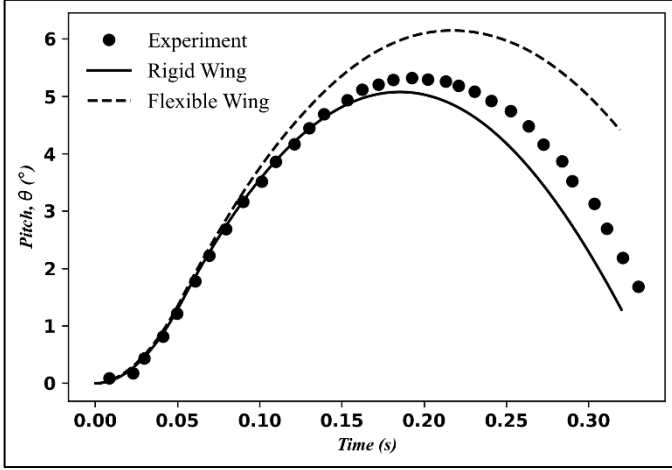


Figure 13: Pitch versus Time graph comparing Flexible and Rigid Wing

The rolling motion of the rigid wing shows much proximity to the experimental results as compared with the flexible wing. The yaw motion for the flexible wing case and rigid wing case shows a similar trend with respect to each other. This is also due to the assumed stiffness of the flexible wing taken. The rigid wing case shows a close match with the experimental case which too has some amount of unknown stiffness. However, if the stiffness of the wing for the flexible case matched the stiffness of the wing of the experimental case, the discrepancy could have been avoided which is also a scope of work in the future.

An aeroelastic test can be performed as a further scope of this study to ascertain the effects of wing stiffness.

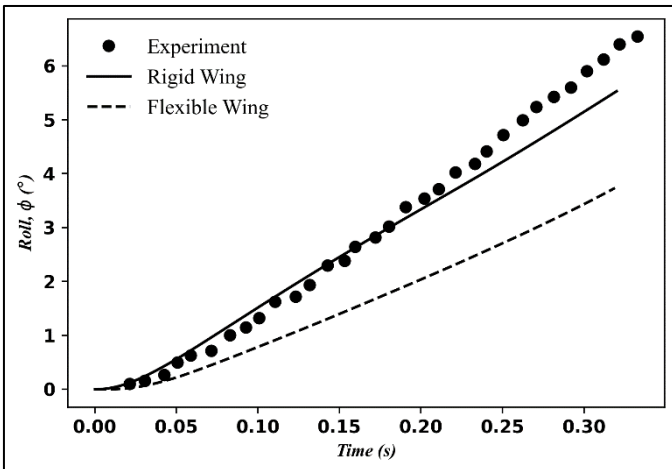


Figure 14: Roll versus Time graph comparing Flexible and Rigid Wing

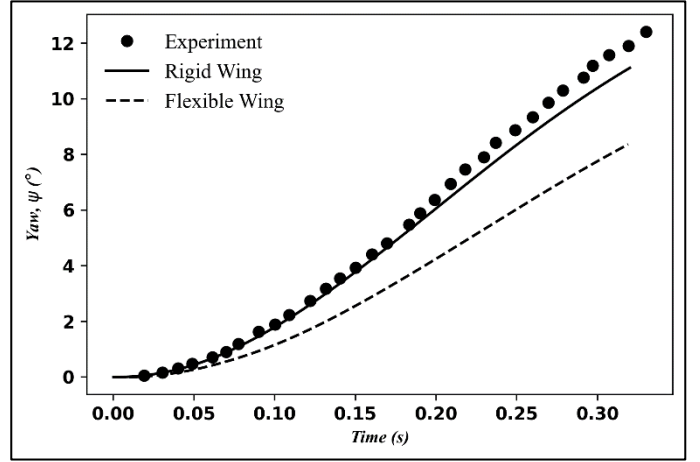


Figure 15: Yaw versus Time graph comparing Flexible and Rigid Wing

5. CONCLUSIONS

Numerical analysis using the Eglin Test Model for the flexible and rigid wing cases successfully shows that there is a deviation in the trajectory of the store for the flexible wing case when compared to the trajectory of the store for the rigid wing case. This paper provides scope to perform this Multiphysics simulation with a validated wing stiffness that is obtained either through experimental investigation of a physical model or from additional literature. Additionally, grid-independent studies are ongoing for this analysis and may show changes in the values of the trajectories for the store. Multiphysics computational analyses similar to the one performed in this study help predict real-world flight conditions, ease the testing during weapon integration, reduce costs and time, improve accuracy, and thereby reduce the risk involved in the testing operations.

ACKNOWLEDGEMENT

We would like to express our token of gratitude to Dr. Karthik Sundarraj, Shripathi V., Sakujiro Hatazawa, and Sachin Pande for their constant support.

A special thanks to Hexagon Manufacturing Intelligence for providing this opportunity to conduct this study.

REFERENCES

- [1] H. Ö. Demir, B. T. Selimhocaoglu, and N. Alemdaroglu, "CFD Applications in Store Separation Gökem DEMİR."
- [2] E. E. Panagiotopoulos and S. D. Kyparissis, "CFD Transonic Store Separation Trajectory Predictions with Comparison to Wind Tunnel Investigations."

- [3] Y. E. Sunay, E. Gülay, and A. Akgül, “Numerical Simulations of Store Separation Trajectories Using the EGLIN Test,” 2013.
- [4] Madasamy S, Thilagapathy G, and Arulalagan R, “Investigation of Store Separation and Trajectory of Weapons in Military Aircraft,” *International Journal of Scientific & Engineering Research*, vol. 7, no. 2, 2016, [Online]. Available: <http://www.ijser.org>
- [5] “E. HEIM, ‘CFD Wing/Pylon/Finned Store Mutual Interference Wind Tunnel Experiment’, Arnold Engineering Development Center, AD-B152 669, September 10-17 1990
- [6] J. Donea, A. Huerta, J.-P. Ponthot, and A. Rodríguez-Ferran, “Chapter 14 Arbitrary Lagrangian-Eulerian Methods”.
- [7] H. K. Versteeg and W. Malalasekera, “Conservation laws of fluid motion and boundary conditions,” *An introduction to computational fluid dynamics: the finite volume method*, vol. M, pp. 9–38, 2007, Accessed: May 11, 2022. [Online]. Available: <http://www.mie.utoronto.ca/labs/mussl/cfd20.pdf>
- [8] “Hexagon MI Documentation Center.” https://help.hexagonmi.com/bundle/MSC_Nastran_2021.3/page/Nastran_Combined_Book/non_linear/ch01/TOC.MSC.Nastran.Documentation1.xhtml (accessed Aug. 15, 2022).
- [9] “Hexagon MI Documentation Center.” https://help.hexagonmi.com/bundle/MSC_Nastran_2021.2/page/Nastran_Combined_Book/qrg/bulkc2/TOC.CTRIA6.xhtml (accessed Aug. 15, 2022).
- [10] “CoSim 2021 - Online Help (HTML).” https://help.hexagonmi.com/bundle/cosim_2021/page/cosim_main.htm (accessed Aug. 15, 2022).
- [11] “scFLOW User’s Guide Analysis Method - 04/Nov/2021.”
- [12] M. Sheharyar, E. Uddin, Z. Ali, Q. Zaheer, and A. Mubashar, “Simulation of a standard store separated from generic wing,” *Journal of Applied Fluid Mechanics*, vol. 11, no. 6, pp. 1579–1589, 2018, doi: 10.29252/jafm.11.06.28865.